

STEADY CREEP OF CIRCULAR CYLINDRICAL SHELLS UNDER COMBINED LATERAL AND AXIAL PRESSURES

R. SANKARANARAYANAN

Hindustan Aeronautics Ltd., Bangalore, India

Abstract—The present paper is concerned with studying the steady creep behaviour of thin circular cylindrical shells subjected to combined lateral and axial pressures. The analysis is based on the Tresca Criterion and the associated flow rule. In order to simplify the analysis, it is assumed that the wall of the shell is made of an ideal sandwich section. It is assumed that the creep rate is the product of a power function of a stress and a function of time. The stresses and deformations are plotted for various values of the parameters of the problem.

1. INTRODUCTION

THE creep stress analysis of thin cylindrical shells has been the subject of several recent investigations. Onat and Yuksel [1] studied the creep behaviour of simply supported sandwich circular cylindrical shells made of Tresca material. Cozzarelli, Patel and Venkatraman [2] have obtained the creep stresses and deformations of clamped sandwich cylindrical shells using the Mises criterion. Based on the square interaction curve [3] the creep stress analysis of simply supported and clamped cylindrical shells [4, 5] was considered by the present author. All these papers are concerned with cylindrical shells without end load. For such shells, the axial force is zero and the axial displacement is of no intrinsic interest. Hence it was sufficient to restrict the consideration to the interaction between the axial bending moment and the circumferential force. If the shell is subjected to both radial and axial forces, the axial force also comes into play and three stress resultants have to be considered rather than two. The present paper is concerned with finding the stresses and deformations of circular cylindrical shells under combined lateral and axial pressures.

Two problems have been investigated. First, circular cylindrical shells under hydrostatic pressure are considered. Subsequently, the analysis is extended to cantilever shells under combined lateral and axial pressures. The material of the shell is assumed to obey the Tresca's criterion and the associated flow rule. In order to simplify the analysis, it is assumed that the wall of the shell is made of an ideal sandwich section consisting of two thin sheets separated by a core which is infinitely strong in shear but can carry no membrane stress. It is assumed that the creep rate is the product of a power function of stress and a function of time. From the outset, consideration will be limited to quasi-steady-state creep processes under constant uniform temperature. Thus the strain at any given instant is assumed to be only a function of stress. A law of this form is frequently a good approximation over at least the secondary creep range, and is valid for many materials whenever the total strain is large enough for the elastic and primary creep effects to be neglected. The problem is regarded as an instantaneous problem in strain rate and the process of integration to determine the total strain is ignored.

2. BASIC EQUATIONS

A. Shells under hydrostatic pressure

The governing equations for the present investigation are expressed in terms of the stress resultants of the shell, whose material has a tensile yield stress λ_0 . The shell (Fig. 1) is of uniform thickness $2H$ and has a radius A and a length $2L$. The bending moment

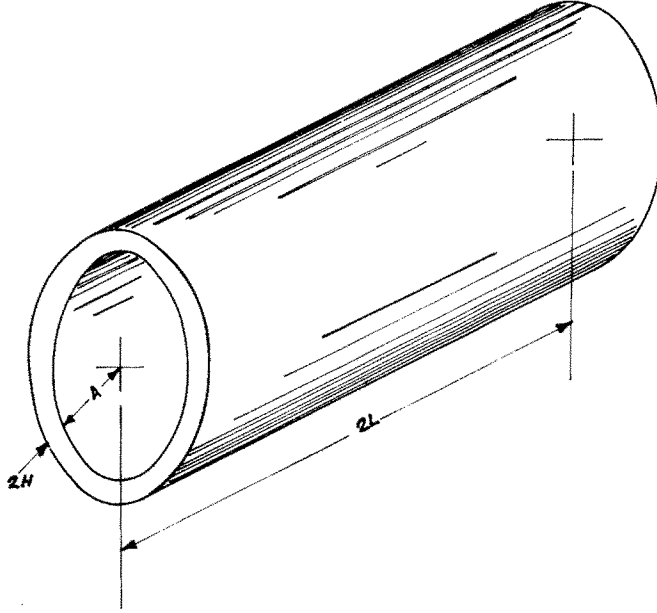


FIG. 1. Dimensions of circular cylindrical shell.

per unit length produced by axial stress is M_x ; the axial and circumferential forces per unit length are given by N_x and N_ϕ respectively. If M_x , N_x and N_ϕ are treated as generalized stress variables, the corresponding strain variables are the curvature of the middle surface κ_x and the strains ϵ_x and ϵ_ϕ . The axial and the inward radial displacements are denoted by U and W , and the axial coordinate X is measured from the built-in end of the shell. The shell is assumed to be subjected to a uniform hydrostatic pressure P .

For the analysis of the present paper, the following dimensionless quantities prove convenient:

$$\begin{aligned}
 x &= \frac{X}{L}; & c^2 &= \frac{L^2}{AH}; & w &= \frac{W}{A}; & u &= \frac{U}{L}; \\
 n_x &= \frac{N_x}{N_0} = \frac{N_x}{2\lambda_0 H}; & m_x &= \frac{M_x}{M_0} = \frac{M_x}{\lambda_0 H^2}; & & & & (2.1) \\
 n_\phi &= \frac{N_\phi}{N_0}; & p &= \frac{PA}{2\lambda_0 H}; & \bar{c} &= \sqrt{2}.
 \end{aligned}$$

Within the framework of the small deformation theory of shells, the governing equations of equilibrium [6] become

$$n'_x = 0; \quad \frac{m''_x}{(\bar{c})^2} + n_\phi + p = 0. \quad (2.2a, b)$$

Primes denote differentiation with respect to the dimensionless axial distance x . The generalized strain rates and the velocities are related by

$$\dot{\epsilon}_x = \dot{u}'; \quad \dot{\epsilon}_\phi = -\dot{w}; \quad \dot{\kappa}_x = -\frac{\dot{w}''}{(\bar{c})^2}. \quad (2.3)$$

The plastic yield condition for an axially symmetric cylindrical shell based on the Tresca criterion has been described by Onat [7]. This yield condition has been replaced by a piecewise linear approximation by Hodge [8] by considering an idealized sandwich shell. The result is a polyhedron defined by twelve planes in the three dimensional stress space with n_x , n_ϕ and m_x as the rectangular cartesian coordinates. Figure 2 shows part of the yield surface which is relevant for the present problem and the corresponding equations of the planes are given in Table 1 [8]. Before we can proceed further, the difference between a plasticity problem and the corresponding creep problem should be

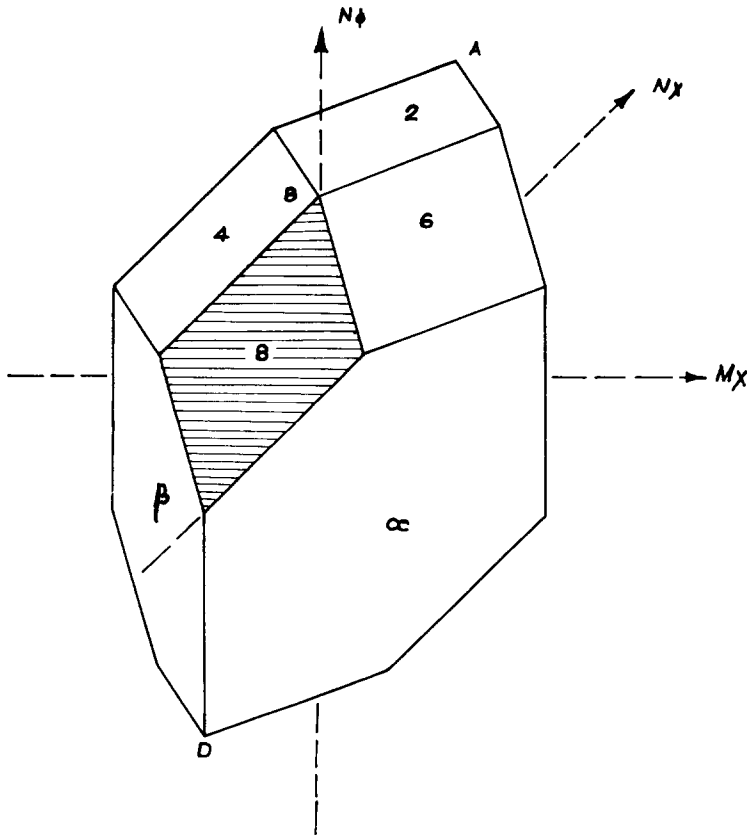


FIG. 2. Linearized interaction surface for circular cylindrical shell.

TABLE 1. FACES AND FLOW RULE FOR YIELD POLYHEDRON FOR CIRCULAR CYLINDRICAL SHELL WITH END LOAD

Face	Equation	Strain rate vector (\dot{u}' , $-\dot{W}'$, $-\dot{w}''/\bar{c}^2$)
1	$-n_\phi = 1$	$\psi(0, -1, 0)$
α	$-n_x + m_x = 1$	$\psi(-1, 0, 1)$
β	$-n_x - m_x = 1$	$\psi(-1, 0, -1)$

stated. A shell will become plastic only if we can find a combination of the generalized stresses such that the stress point is in contact with the yield surface. However, creep can take place at any level of stress. A family of creep loci for the circular cylindrical shells is indicated in Fig. 3.

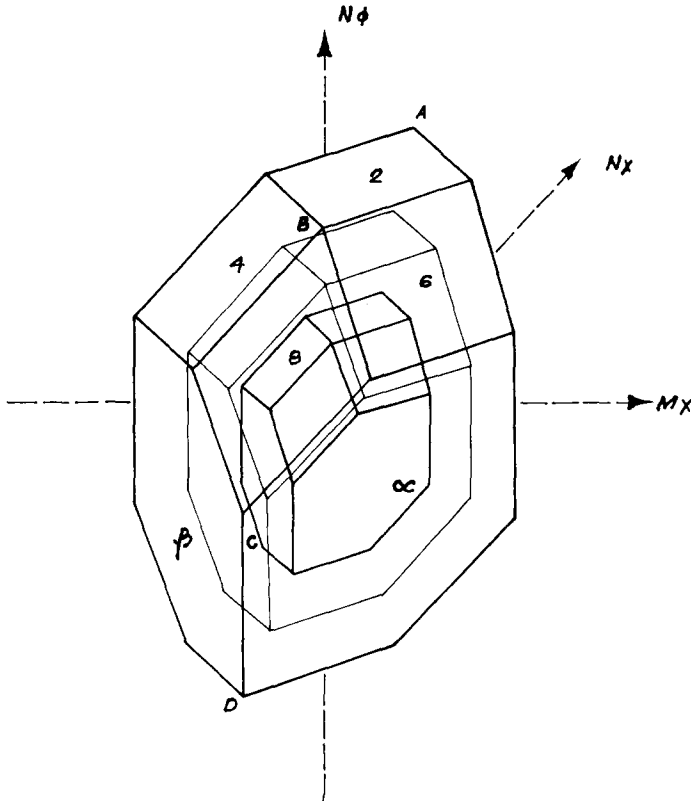


FIG. 3. Creep interaction surface of a circular cylindrical shell.

Let us consider a typical formulation of the creep law on the basis of the polyhedron Fig. 2. In regime 1, $\dot{\epsilon}_x = \dot{\kappa}_x = 0$ and the rate of dissipation of mechanical energy becomes

$$U = n_\phi \dot{\epsilon}_\phi = QF(Q)G(t). \tag{2.4}$$

Hence

$$Q = n_\phi; \quad \dot{\epsilon}_\phi = F(Q)G(t). \quad (2.5)$$

Similar results can be obtained for the other regimes and are given in Ref. [4]. The creep laws relevant to the present problem are given in Table 2. The analysis has been carried out on the assumption that $F(Q)$ is a power function of the generalized stress.

$$F(Q) = (Q/\mu)^n \quad (2.6)$$

where n and μ are constants depending on the material and the temperature.

TABLE 2. CREEP LAWS FOR CIRCULAR CYLINDRICAL SHELL WITH END LOAD

Faces	Generalized forces	Generalized strain rates	Creep law
1	$Q = -n_\phi > 0$	$\dot{\epsilon}_\phi \leq 0; \quad \dot{\epsilon}_x = \dot{\kappa}_x = 0$	$\dot{\epsilon}_\phi = -F(Q)G(t)$
1, α	$Q = -n_\phi = -n_x + m_x > 0$	$\dot{\epsilon}_\phi \leq 0; \quad \dot{\epsilon}_x \leq 0;$ $\dot{\kappa}_x \geq 0; \quad \dot{\epsilon}_x + \dot{\kappa}_x = 0$	$\dot{\kappa}_x - \dot{\epsilon}_\phi = F(Q)G(t)$
1, β	$Q = -n_\phi = -n_x - m_x > 0$	$\dot{\epsilon}_\phi \leq 0; \quad \dot{\epsilon}_x = \dot{\kappa}_x \leq 0$	$\dot{\kappa}_x + \dot{\epsilon}_\phi = -F(Q)G(t)$

The boundary conditions for the problem are

$$\text{at } x = 0, \quad \dot{w}(0) = \dot{w}'(0) = 0 \quad (2.7)$$

$$\text{at } x = 1, \quad \dot{u}(1) = \dot{w}'(1) = m'_x(1) = 0 \quad (2.8)$$

$m_x, m'_x, n_\phi, \dot{u}, \dot{w}$ and \dot{w}' must be continuous throughout the shell.

B. Shells under combined lateral and axial pressures

We consider a shell clamped at one end and free at the other as shown in Fig. 4. The shell is subjected to a uniform lateral pressure P and at the same time the free end of the shell

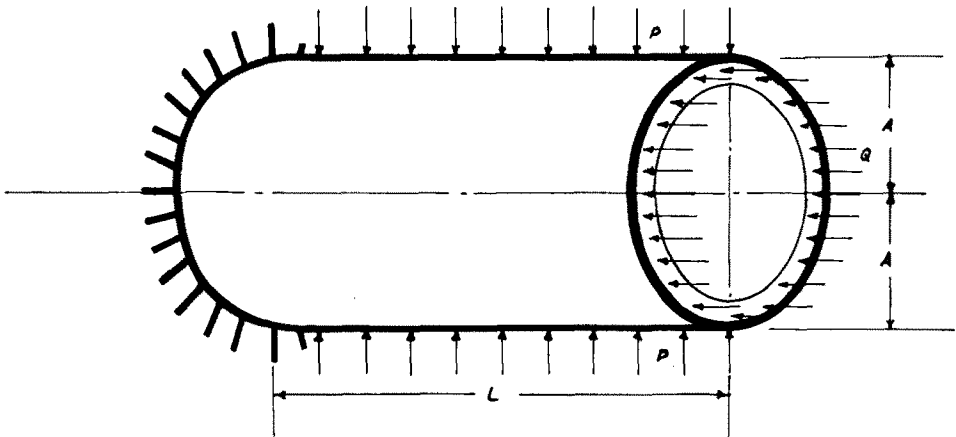


FIG. 4. Shell clamped at one end and free at the other.

is subjected to an axial pressure Q . The shell is of uniform thickness $2H$, has a radius A and a length L . In addition to the dimensionless quantities given by equation (2.1) we further define

$$q = QA/2\lambda_0 H. \quad (2.9)$$

The equations of equilibrium (2.2a, b) are directly applicable for this case also. However, the boundary conditions for this problem are

$$\text{at } x = 0, \quad \dot{u}(0) = \dot{w}(0) = \dot{w}'(0) = 0 \quad (2.10)$$

$$\text{at } x = 1, \quad m_x(1) = m'_x(1) = 0, \quad n_x(1) = -q/2. \quad (2.11)$$

As stated previously m_x , m'_x , n_ϕ , \dot{u} , \dot{w} and \dot{w}' must be continuous throughout the shell.

3. SOLUTION

A. Shells under hydrostatic pressure

Let us first consider a clamped shell in a hydrostatic pressure field. The initial choice of the stress profile is motivated by the physical considerations of the problem. Physically it is reasonable to expect the hoop stress to be everywhere compressive, so that $n_\phi < 0$.

As a first hypothesis we shall assume that the entire stress profile lies on regime 1. Since $\dot{\kappa}_x = 0$ in regime 1, \dot{w} must be a linear function of x . Application of the Boundary conditions (2.7) and (2.8) implies no displacement at all and the shell would remain rigid, a result which is not acceptable. An acceptable hypothesis can be formulated by modifying the stress profile near the shell edges $x = 0$ and $x = 1$. The simplest possible hypothesis is a two piece stress profile; a finite portion $0 \leq x \leq \rho$ of the shell is at the intersection of regimes 1 and β and the remainder $\rho \leq x \leq 1$ of the shell is at the intersection of regimes 1 and α , Fig. 5(a). The solution under this hypothesis is given below :

$0 \leq x \leq \rho$:

$$\frac{m_x}{p} = \frac{1}{2}[\cos \bar{c}(\rho - x) - \tanh \bar{c}(1 - \rho) \sin \bar{c}(\rho - x) - 1] \quad (3.1)$$

$$\frac{m'_x}{p} = \frac{\bar{c}}{2}[\sin \bar{c}(\rho - x) + \tanh \bar{c}(1 - \rho) \cos \bar{c}(\rho - x)] \quad (3.2)$$

$$\frac{n_\phi}{p} = -\left\{1 - \frac{1}{2}[\cos \bar{c}(\rho - x) - \tanh \bar{c}(1 - \rho) \sin \bar{c}(\rho - x)]\right\} \quad (3.3)$$

$$\frac{\dot{w}'}{G(\bar{c})^2(p/\mu)^n} = \int_0^x [\cos \bar{c}(x - \xi)] \left\{1 - \frac{1}{2}[\cos \bar{c}(\rho - \xi) - \tanh \bar{c}(1 - \rho) \sin \bar{c}(\rho - \xi)]\right\}^n d\xi \quad (3.4)$$

$$\frac{\dot{w}}{G\bar{c}(p/\mu)^n} = \int_0^x [\sin \bar{c}(x - \xi)] \left\{1 - \frac{1}{2}[\cos \bar{c}(\rho - \xi) - \tanh \bar{c}(1 - \rho) \sin \bar{c}(\rho - \xi)]\right\}^n d\xi \quad (3.5)$$

$$\dot{u} = -\frac{\dot{w}'}{(\bar{c})^2}. \quad (3.6)$$

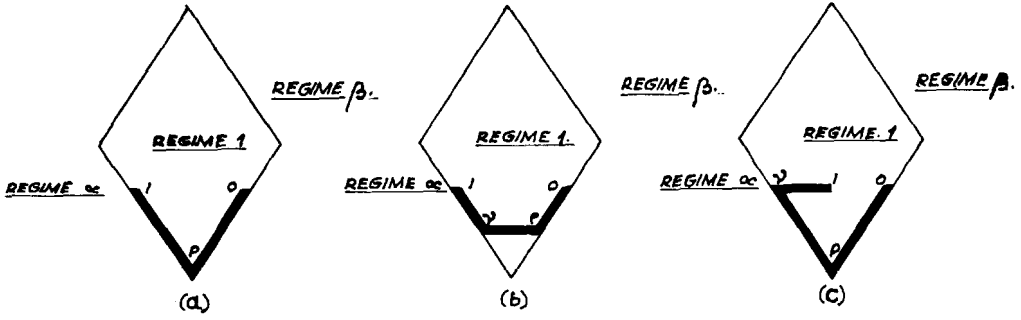


FIG. 5. Stress profiles for circular cylindrical shell under hydrostatic pressure.

$$\underline{\rho \leq x \leq 1:}$$

$$\frac{m_x}{p} = \frac{1}{2} \left[1 - \frac{\cosh \bar{c}(1-x)}{\cosh \bar{c}(1-\rho)} \right] \quad (3.7)$$

$$\frac{m'_x}{p} = \frac{\bar{c}}{2} \left[\frac{\sinh \bar{c}(1-x)}{\cosh \bar{c}(1-\rho)} \right] \quad (3.8)$$

$$\frac{n_\phi}{p} = - \left\{ 1 - \frac{1}{2} \left[\frac{\cosh \bar{c}(1-x)}{\cosh \bar{c}(1-\rho)} \right] \right\} \quad (3.9)$$

$$\begin{aligned} \frac{\dot{w}'}{G(\bar{c})^2(p/\mu)^n} &= \int_0^\rho [\cos \bar{c}(\rho - \xi) \cosh \bar{c}(x - \rho) + \sin \bar{c}(\rho - \xi) \sinh \bar{c}(x - \rho)] \\ &\quad \times \left\{ 1 - \frac{1}{2} [\cos \bar{c}(\rho - \xi) - \tanh \bar{c}(1 - \rho) \sin \bar{c}(\rho - \xi)] \right\}^n d\xi \\ &\quad - \int_\rho^x [\cosh \bar{c}(x - \xi)] \left[1 - \frac{1}{2} \frac{\cosh \bar{c}(1 - \xi)}{\cosh \bar{c}(1 - \rho)} \right]^n d\xi \end{aligned} \quad (3.10)$$

$$\begin{aligned} \frac{\dot{w}}{G\bar{c}(p/\mu)^n} &= \int_0^\rho [\cos \bar{c}(\rho - \xi) \sinh \bar{c}(x - \rho) + \sin \bar{c}(\rho - \xi) \cosh \bar{c}(x - \rho)] \\ &\quad \times \left\{ 1 - \frac{1}{2} [\cos \bar{c}(\rho - \xi) - \tanh \bar{c}(1 - \rho) \sin \bar{c}(\rho - \xi)] \right\}^n d\xi \\ &\quad - \int_\rho^x [\sinh \bar{c}(x - \xi)] \left[1 - \frac{1}{2} \frac{\cosh \bar{c}(1 - \xi)}{\cosh \bar{c}(1 - \rho)} \right]^n d\xi \end{aligned} \quad (3.11)$$

$$\begin{aligned} \frac{\dot{u}}{2G(p/\mu)^n} &= \frac{\dot{w}'}{2G(\bar{c})^2(p/\mu)^n} - \int_0^\rho [\cos \bar{c}(\rho - \xi) \{ 1 - \frac{1}{2} [\cos \bar{c}(\rho - \xi) \\ &\quad - \tanh \bar{c}(1 - \rho) \sin \bar{c}(\rho - \xi)] \}^n d\xi. \end{aligned} \quad (3.12)$$

ρ has to be determined from the following equation

$$\begin{aligned} &\int_0^\rho [\cos \bar{c}(\rho - \xi) + \tanh \bar{c}(1 - \rho) \sin \bar{c}(\rho - \xi)] \\ &\quad \times \left\{ 1 - \frac{1}{2} [\cos \bar{c}(\rho - \xi) - \tanh \bar{c}(1 - \rho) \sin \bar{c}(\rho - \xi)] \right\}^n d\xi \\ &= \int_0^1 \left[\frac{\cosh \bar{c}(1 - \xi)}{\cosh \bar{c}(1 - \rho)} \right] \left\{ 1 - \frac{1}{2} \left[\frac{\cosh \bar{c}(1 - \xi)}{\cosh \bar{c}(1 - \rho)} \right] \right\}^n d\xi. \end{aligned} \quad (3.13)$$

For given values of n and c , the integral equation (3.13) is numerically solved for ρ . Once ρ is known as a function of n and c the stresses and deformations are obtained from equations (3.1) to (3.12).

Equations (3.1) to (3.13) are based on certain assumptions regarding the stress profile of the shell. It now remains to determine the conditions under which the above solution is admissible. In order to do this, a value of n is fixed and c is gradually increased from a very small value. The corresponding values of the stresses, deflections and their slopes are calculated and these are examined to see whether the relevant inequalities are satisfied. If they are satisfied, another value of c is assumed for the same value of n and the process repeated. Proceeding in this manner it is found that there are two types of violations for different combinations of n and c . For intermediate values of c the violation takes place in the neighbourhood of $x = \rho$ of the shell simultaneously in both the regimes.

$$0 \leq x \leq \rho : \dot{\kappa}_x \leq 0 \tag{3.14a}$$

$$\rho \leq x \leq 1 : \dot{\kappa}_x \geq 0. \tag{3.14b}$$

For large values of c and relatively small values of n , the boundary condition (2.8) is violated near $x = 1$. Let us first restrict our attention to the violation taking place in the neighbourhood of $x = \rho$ of the shell.

The limiting value of c_L of c for the assumed value of n for which the solution given by equations (3.1) to (3.13) is admissible is found numerically. Now another value of n is assumed and the process is repeated. It is again found that there exists a limiting value c_L of c such that for values of $c \leq c_L$ all the appropriate inequalities are satisfied and for values of $c > c_L$ the Inequalities (3.14a, b) are violated. The limiting values of n and c delineate a regime in the n - c plane, Fig. 6 which is designated as regime I. Figures 7 (a, b, c and d) show the stresses and deformations for the case $c = 0.5$ for different values of n .

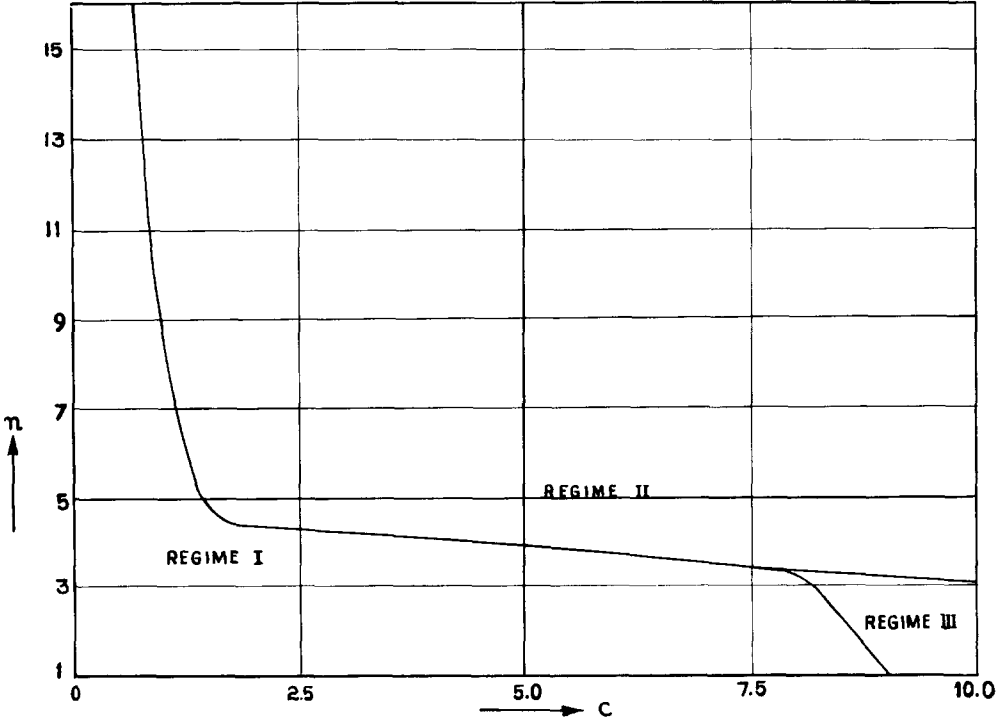


FIG. 6. Range of validity of the different solutions.

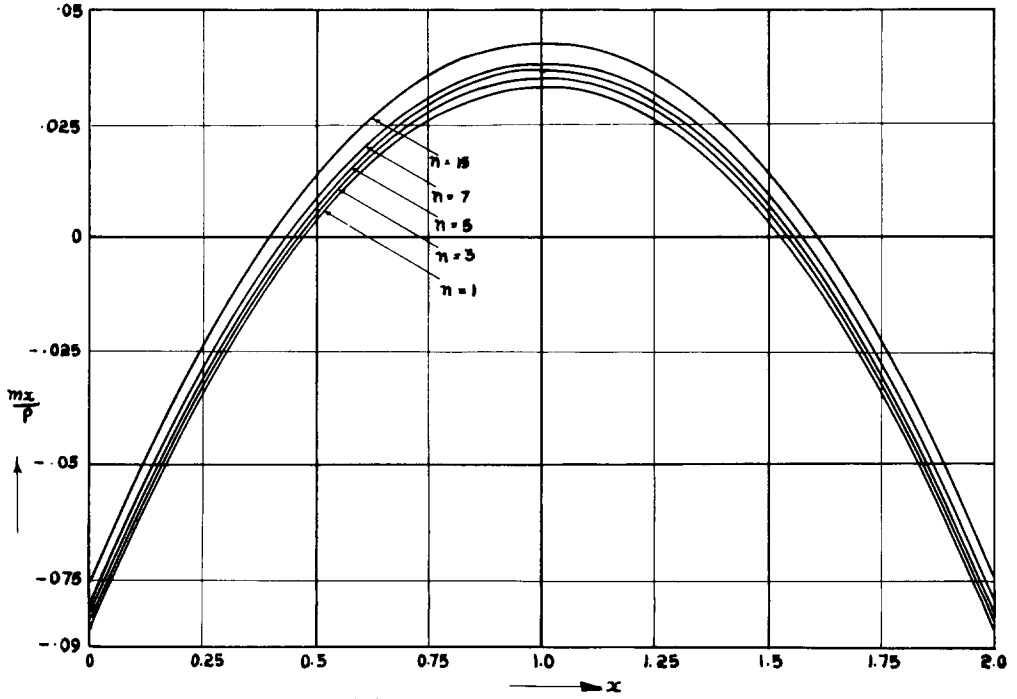


FIG. 7(a). Axial bending moment distribution, $c = 0.5$.

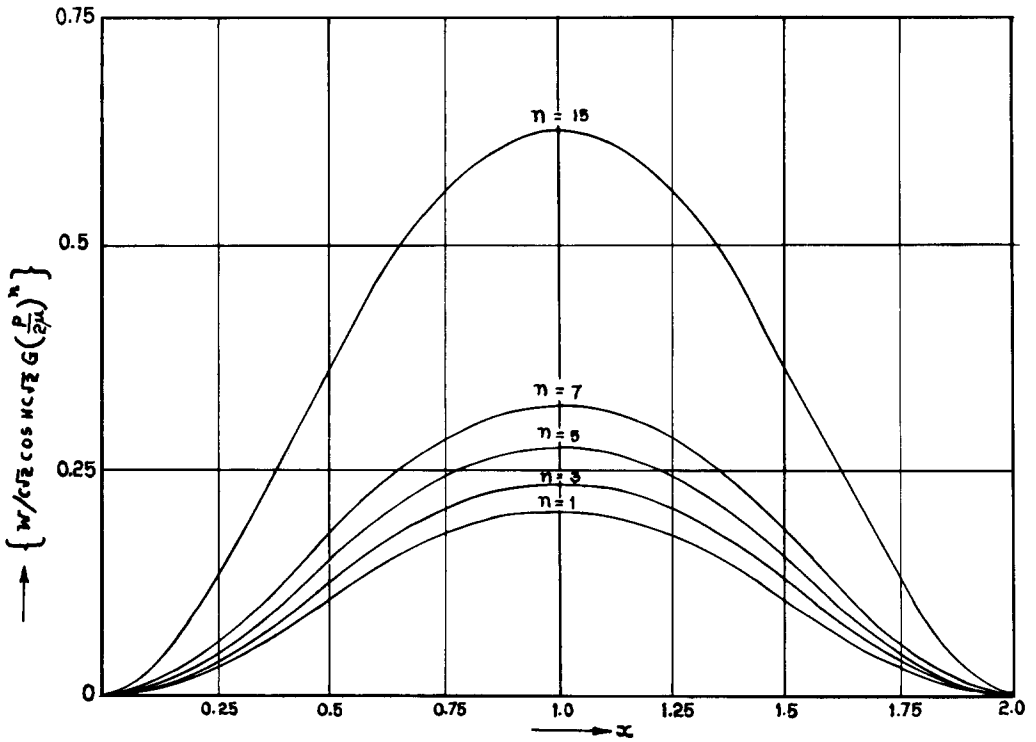


FIG. 7(b). Radial deformation rate, $c = 0.5$.

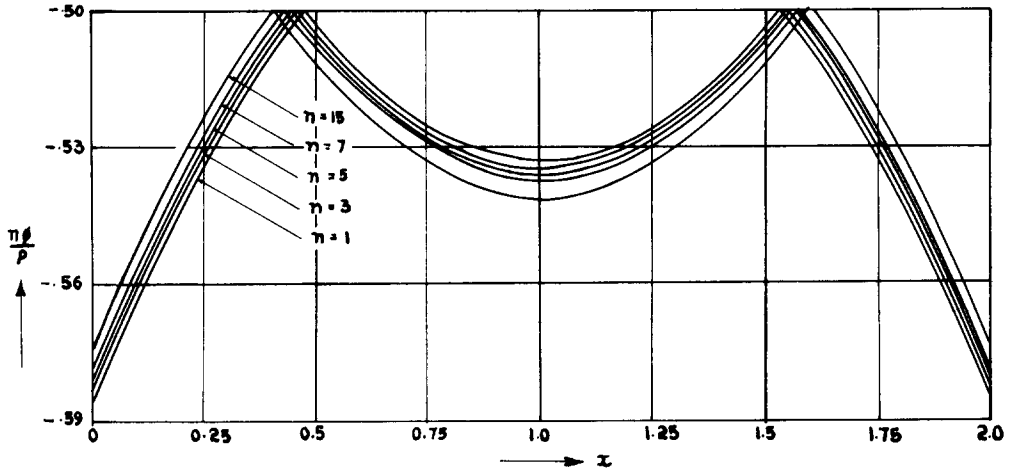


FIG. 7(c). Circumferential force distribution, $c = 0.5$.

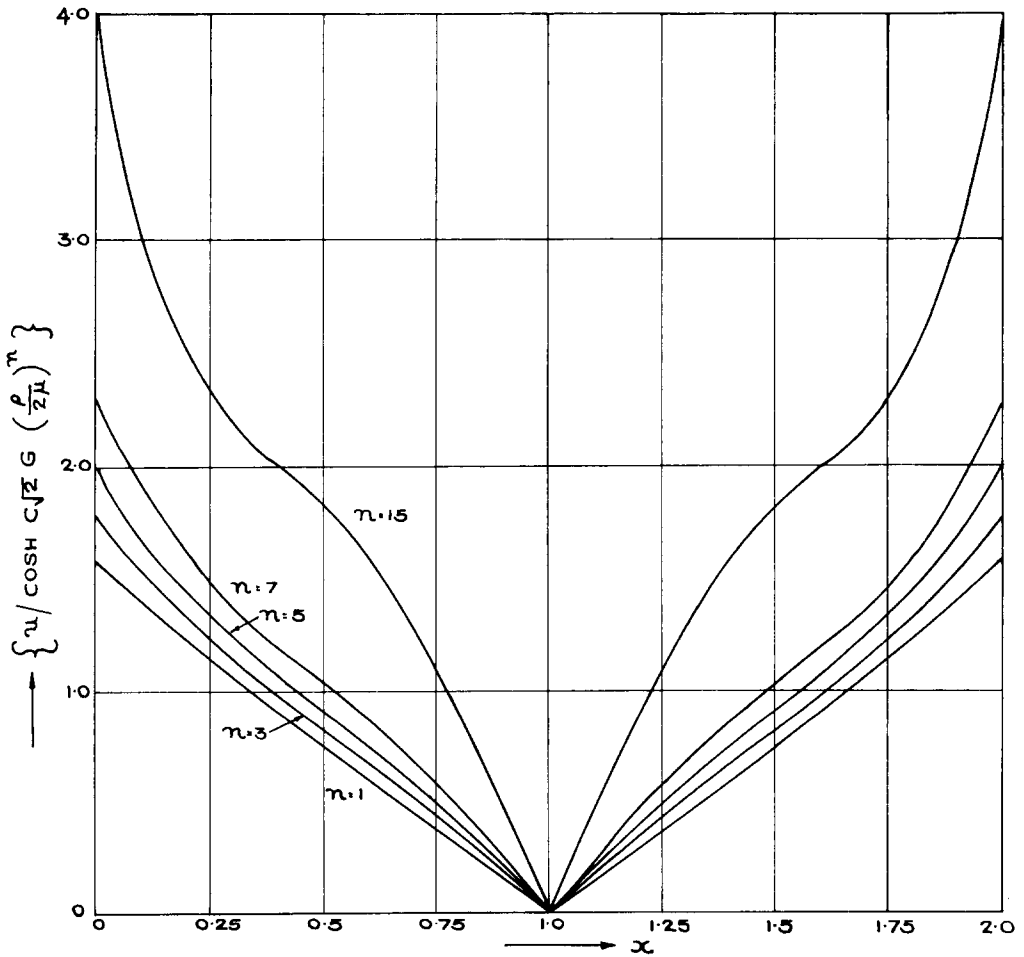


FIG. 7(d). Axial deformation rate, $c = 0.5$.

For values of n and c which lie off the regime I, it appears reasonable to modify the preceding stress profile such that $\kappa_x = 0$ for a finite portion of the shell near $x = \rho$. An examination of Table 2 shows that in regime 1, $\kappa_x = 0$. This suggests the following stress profile, Fig. 5(b).

$$0 \leq x \leq \rho: \quad \text{Intersection of 1 and } \beta \tag{3.15a}$$

$$\rho \leq x \leq v: \quad \text{Regime 1} \tag{3.15b}$$

$$v \leq x \leq 1: \quad \text{Intersection of 1 and } \alpha. \tag{3.15c}$$

The solution under this hypothesis is worked out from Table 2 and equations (2.2), (2.6), (2.7), and (2.8). For the sake of brevity, the details are not included in this paper and the interested reader can get them from Ref. [11]. The range of validity of the preceding solution is numerically established and it is found that all the appropriate inequalities are satisfied in the region designated as regime II in Fig. 6. The preceding solution indicated a violation of the boundary condition equation (2.8), namely $\dot{w}'(1) = 0$ for large values of c and relatively small values of n . This suggests a stress profile as shown in Fig. 5(c). Since the analysis is very similar to the one described above we refrain ourselves from presenting further details of the solution.

It is verified that the solution corresponding to the stress profile, Fig. 5(c) satisfies all the appropriate inequalities in the region designated as regime III in Fig. 6.

B. Shells under combined lateral and axial pressures

For the cantilever shell, the equilibrium equation (2.2a) and the boundary condition (2.11) show that the axial stress is given by

$$n_x = -q/2. \tag{3.16}$$

The analysis of this problem follows very closely to the one detailed in Section A. Hence this problem will be discussed only briefly. Reasoning in a manner similar to that given in Section A, the simplest stress profile appears to be the one shown in Fig. 8(a). The solution corresponding to the above stress profile should satisfy the following inequalities.

$$0 \leq x \leq 1:$$

$$-n = -n_x - m_x > 0; \quad m_x < 0; \tag{3.17}$$

$$\dot{\epsilon}_\phi \leq 0; \quad \dot{\epsilon}_x = \dot{\kappa}_x \leq 0. \tag{3.18}$$

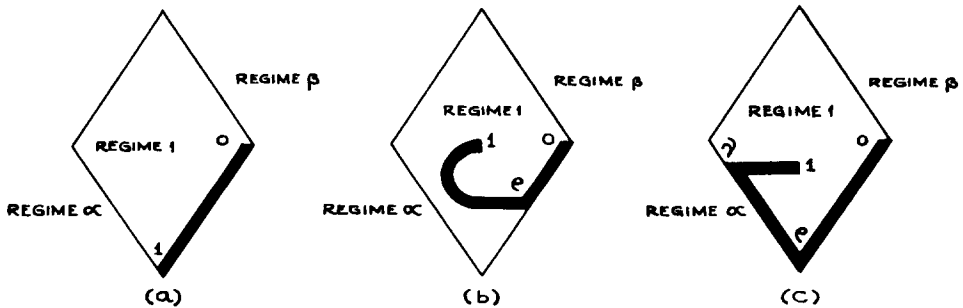


FIG. 8. Stress profiles for circular cylindrical shell under combined lateral and axial pressures.

It is found that Inequality (3.18), namely $\dot{\kappa}_x < 0$ is satisfied only for a limited number of values of n and c . The range of validity of the above solution is delineated as regime I in Fig. 9. For values of n and c which lie off the regime I, it seems appropriate to try the stress profile shown in Fig. 8(b). The corresponding inequalities are

$$\underline{0 \leq x \leq \rho:}$$

$$-n = -n_x - m_x > 0; \quad m_x < 0; \quad (3.19)$$

$$\dot{\epsilon}_\phi \leq 0; \quad \dot{\epsilon}_x = \dot{\kappa}_x \leq 0; \quad (3.20)$$

$$\underline{\rho \leq x \leq 1:}$$

$$-n_\phi > 0; \quad (3.21)$$

$$\dot{\epsilon}_\phi \leq 0; \quad \dot{\epsilon}_x = \dot{\kappa}_x = 0. \quad (3.22)$$

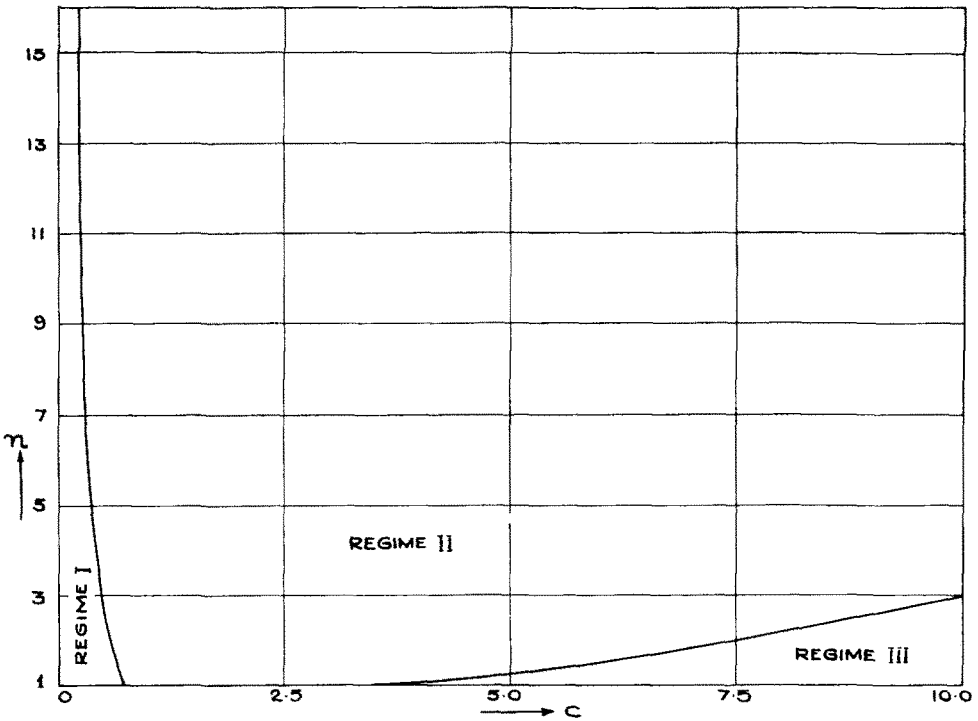


FIG. 9. Range of validity of the different solutions.

In this case it is found that Inequality (3.19), namely $m_x < 0$ is satisfied for values of n and c which lie in regime II of Fig. 9. For values of n and c which violate the condition $m_x < 0$, the stress profile shown in Fig. 8(c) is attempted. The corresponding inequalities are

$$\underline{0 \leq x \leq \rho:}$$

$$-n_\phi = -n_x - m_x > 0; \quad m_x < 0; \quad (3.23)$$

$$\dot{\epsilon}_\phi \leq 0; \quad \dot{\epsilon}_x = \dot{\kappa}_x \leq 0; \quad (3.24)$$

$\rho \leq x \leq v$:

$$-n_\phi = -n_x + m_x > 0; \quad m_x > 0; \quad (3.25)$$

$$\dot{\epsilon}_\phi \leq 0; \quad \dot{\epsilon}_x = -\dot{\kappa}_x \leq 0; \quad (3.26)$$

$v \leq x \leq 1$:

$$-n_\phi > 0; \quad (3.27)$$

$$\dot{\epsilon}_\phi \leq 0; \quad \dot{\epsilon}_x = \dot{\kappa}_x = 0. \quad (3.28)$$

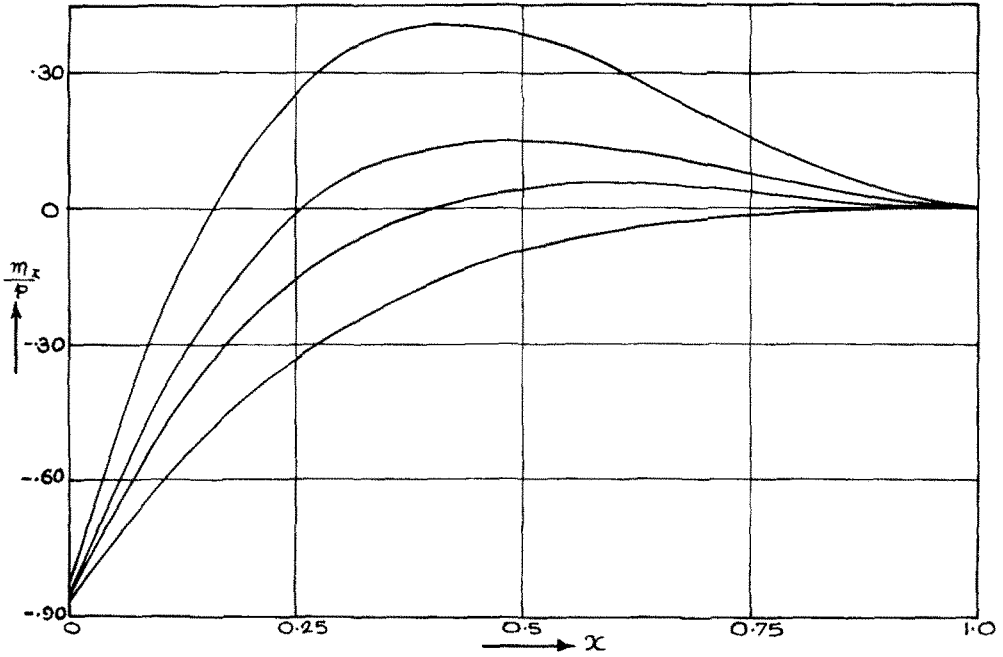


FIG. 10(a). Axial bending moment distribution, $c = 5$.

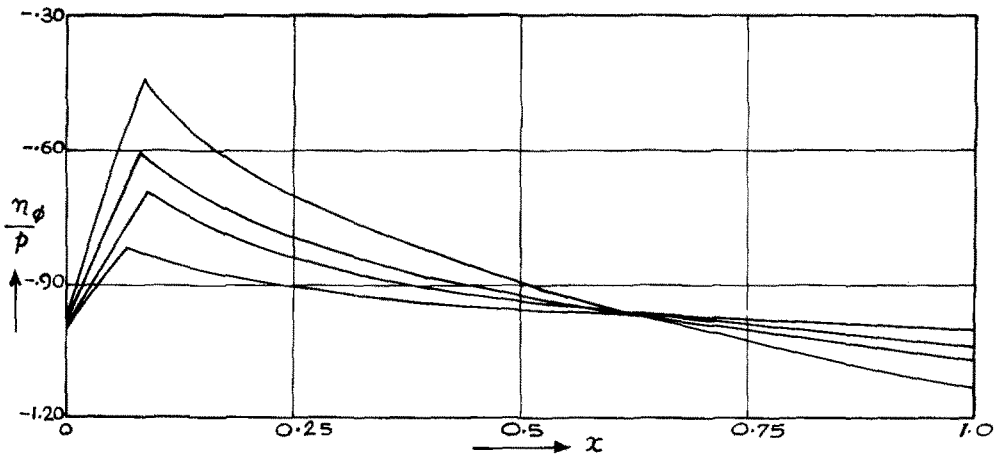


FIG. 10(b). Circumferential force distribution, $c = 5$.

It is numerically verified that these inequalities are satisfied for values of n and c in regime III of Fig. 9. The stress resultants and the deformation rates for the case $c = 5$ are presented in Figs. 10 (a, b, c, d).

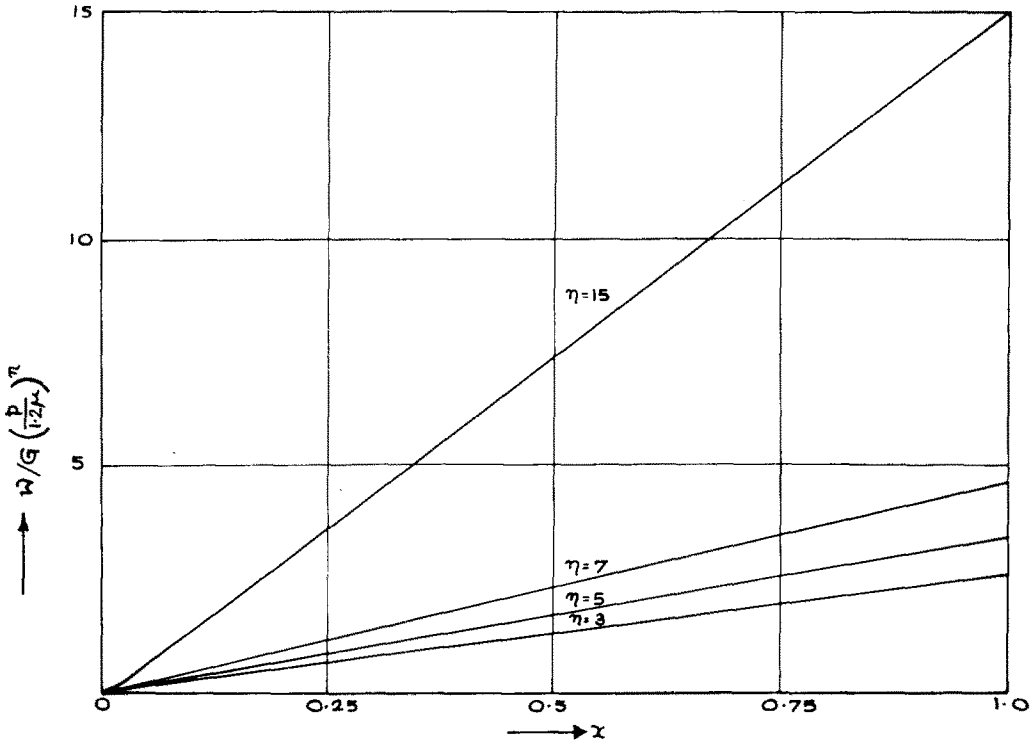


FIG. 10(c). Radial deformation rate, $c = 5$.

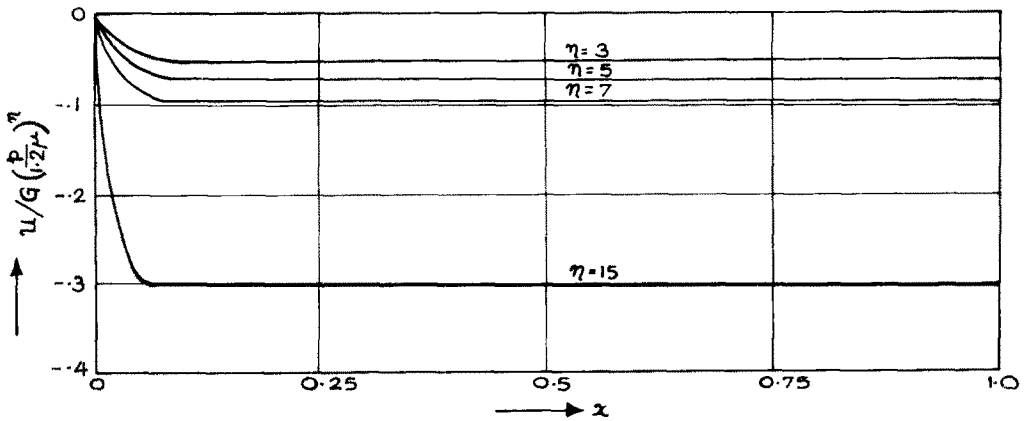


FIG. 10(d). Axial deformation rate, $c = 5$.

4. CONCLUSION

There are two factors which often cause considerable difficulty in solving problems of creep stress analysis. The first is essentially lack of adequate creep data, due to the innate variability of the creep properties of a material. The second factor is the analytical difficulty of determining the stresses and deformations of a given structure for an arbitrary creep law. The solution to both problems is essentially the same. Simplified creep laws must be chosen to enable analytical or numerical solutions to be obtained. Even though the choice of the creep law is to some extent arbitrary, it must be chosen in such a manner that in the first case the effect of the uncertainty in the creep data is minimized and in the second case the simplified law gives a good approximation for the creep stresses and deformations. In this paper, an attempt has been made to overcome some of the analytical difficulties by replacing the non-linear function by a piecewise linear approximation and the method is applied to studying the steady creep behaviour of circular cylindrical shells.

Considerable caution should be exercised before interpreting the above results for actual shells. At the present time there is relatively little experimental work available on the creep behaviour of cylindrical shells. The results obtained in this paper must therefore be regarded as tentative.

In the first place it is necessary to assess the effect of replacing the actual criterion by a piecewise linear approximation. In order to do this, it is necessary to investigate a shell problem under the hypotheses of different criteria and to compare the results. Some work is being currently done by the author along these lines and it is hoped that the results will be made available in the near future.

The scope of the paper is limited to quasi-steady-state creep processes under constant uniform temperature. A law of this form is considered to be a good approximation over the secondary creep range and is valid for many materials whenever the total strain is large enough in order to justify the neglect of elastic effects.

The problem considered in the paper is regarded as an instantaneous problem in strain rate, and the process of integration to determine the total strain is ignored.

Neglecting elastic strains and strain-hardening will probably result in only small errors in the predicted results. However, the assumption that the shell continues to be axially symmetric as it deforms, is likely to lead to serious errors. It is probable that instability will occur in some form, and this aspect of the problem has to be investigated.

Despite these limitations, it is hoped that the analysis presented here will be of some use. A final verdict on the validity of the present solution must await further analytical and experimental results.

REFERENCES

- [1] E. T. ONAT and H. YUKSEL, On the steady creep of shells. *Proc. 3rd U.S. natn. Congr. appl. Mech.* ASME, New York, 1958, pp. 625-640.
- [2] F. A. COZZARELLI, S. A. PATEL and B. VENKATRAMAN, Creep analysis of circular cylindrical shells. *AIAA Jnl* 3, 1298-1301 (1965).
- [3] D. C. DRUCKER, Limit analysis of cylindrical shells under axially-symmetric loading. *Proc. 1st Midwestern Conf. Solid Mech.*, Urbana, 1953, pp. 158-163.
- [4] R. SANKARANARAYANAN, Steady creep of plates and shells. *J. aeronaut. Soc. India* 17, 200-219 (1965).
- [5] R. SANKARANARAYANAN, Steady creep of circular cylindrical shells under axially symmetric loading. To be published.
- [6] S. P. TIMOSHENKO, *Theory of Plates and Shells*. McGraw-Hill (1940).
- [7] E. T. ONAT, Plastic collapse of cylindrical shells under axially symmetrical loading. *Q. appl. Math.* 13, 63-72 (1955).

- [8] P. G. HODGE, JR., The rigid-plastic analysis of symmetrically loaded cylindrical shells. *J. appl. Mech.* **21**, 336-342 (1954).
- [9] F. B. HILDERBRAND, *Introduction to Numerical Analysis*. McGraw-Hill (1956).
- [10] P. G. HODGE, JR., *Plastic Analysis of Structures*. McGraw-Hill (1959).
- [11] R. SANKARANARAYANAN, Steady creep of circular cylindrical shell under combined lateral and axial pressures. *HAL tech. Rep.* (1968).

(Received 1 March 1968; revised 10 June 1968)

Абстракт—Настоящая работа касается исследования поведения ползучести тонких, осесимметрических оболочек, подверженных горизонтальным и осевым давлениям.

Анализ основывается на критерии Треска и соответствующим законе течения. Для упрощения анализа принято, что стенка оболочки обладает идеально слоистым сечением. Предлагается, что скорость ползучести является произведением степенной функции напряжения и функции времени. Даются диаграммы для напряжений и деформаций при разных значениях параметров задачи.